Geodynamic processes of the continental subduction

constraints from refine crustal structure beneath the Pamir Plateau

Wei Li[1,2,3] Yun Chen[1,2] Ping Tan[4] Xiaohui Yuan[3]

1 Institute of Geology and Geophysics, Chinese Academy of Sciences, Beijing, China; 2 Innovation Academy for Earth Science, Chinese Academy of Sciences, Beijing, China
3 Deutsches GeoForschungsZentrum GFZ, Telegrafenberg, Potsdam, Germany; 4 Institute of Disaster Prevention, Sanhe, Hebei, China

Introduction

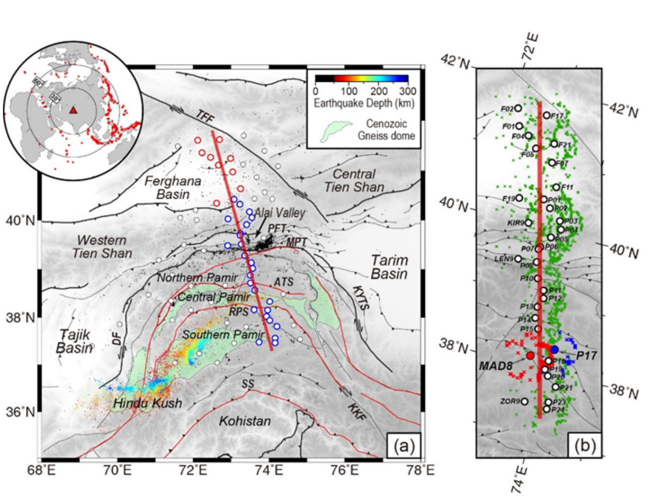

Figure 1 (a) Topographic and tectonic map of the Pamir plateau. Dots show seismicity with different colors denoting different depths (source: Sippl et al., 2013b; Kufner et al., 2017). The upper-left insetmap shows the distribution of events used in this study. The green areas show the locations of Cenozoic gneiss domes. (b) Circles and crosses respectively denote the stations and piercing points of the Ps converted phases at the depth of 60 km.

As a transition from the oceanic subduction to the continental collision, the continental subduction has been proved by ultrahigh-pressure (UHP) rocks in the orogenic belts (Chopin, 1984; Smith, 1984), and promoted a revolution of the plate tectonics (Zheng et al., 2009). However, UHP rocks have experienced complicated exhuming process, and only provide constraints on a small portion of the continental subducting zone in past tectonic events. Such a limited spatial-temporal distribution would restrict the comprehensive understanding of the continental subduction.

The Pamir plateau, located north of the western syntaxis of the India–Eurasia collision system, is featured by the intense intermediate-depth seismicity with a maximum depth down to ~300 km (Figure 1), that is significantly different from the Tibetan plateau, in where the seismicity is shallower than 90 km. In recent years, benefited from several temporary seismic arrays deployed in and around the Pamir plateau, the lithospheric structure and stress-field characteristics in this area have been revealed (Schneider et al., 2013; Sippl et al., 2013a; Kufner et al., 2016; Li et al., 2018b), and indicate that intermediate-depth seismic zones beneath the Pamir and Hindu Kush are triggered by the convergent subduction of the Asian and Indian slabs. Distinguished from other intra-continental intermediate-depth seismic zones where are not far away from an active oceanic subduction zone (McKenzie et al., 2019), the intermediate-depth seismicity beneath Pamir plateau is related to the passive subduction of the Asian continental slab, and therefore, it's an idea place to effectively understand the continental subduction.

In this study, based on dense seismic stations arrayed linearly across the Pamir continental subducting zone, we use the harmonic analysis of receiver functions to minimize the potential influence of the dipping interface and azimuthal anisotropy, and obtain average receiver functions with a resolution coordinate with the surface wave dispersions obtained in the previous ambient noise tomography (Li et al., 2018a). Then, a joint inversion of receiver functions and surface wave dispersions is used to construct a refined model of crust and uppermost mantle beneath the Pamir plateau, and the spatial relationships of structures at different depths are analyzed to provide constraints for the geodynamic process of continental subduction.

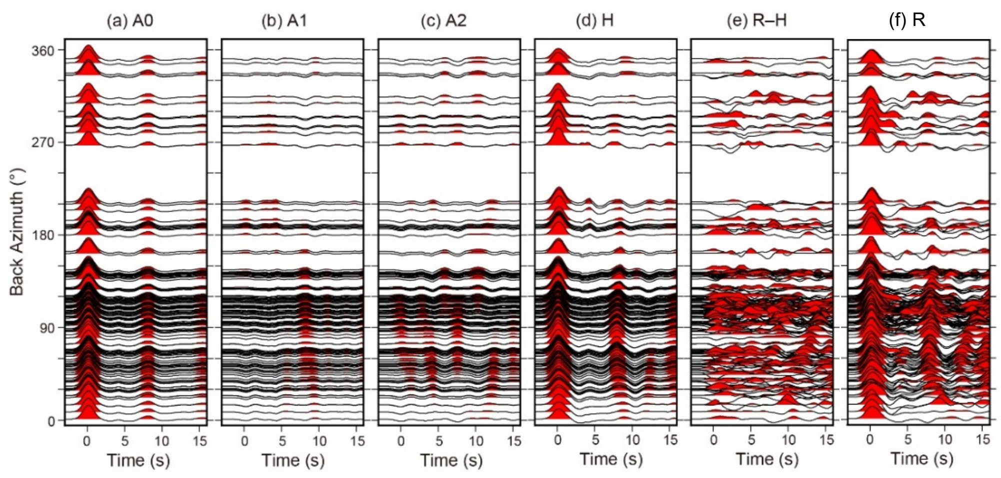

Data

In past decade, several temporary seismic arrays have been conducted in and around the Pamir plateau, including the TIPAGE (Tien shan–PAmir GEodynamic program) covered the main Pamir from 2008 to 2010 and FERGHANA operated in the Tien Shan and Ferghana basin from 2009 to 2010. In this study, based on a 24-stations profile with a 15-km station space from the TIPAGE, we collect other 5 stations from TIPAGE near to the profile, and 8 stations from FERGHANA as a northward extension of the profile, to construct a ~520-km length broadband seismic profile crossed the main tectonic units of the Pamir plateau, Alai valley, western Tien Shan and Ferghana basin (Figure 1).

Figure 2 Example of the harmonic analysis of receiver functions recorded at station MAD8. (a-c) three harmonic components Ai (i = 0, 1, 2) estimated from the harmonic analysis of quality controlled receiver functions dataset of the station MAD8. (d) Harmonic receiver functions H as the sum of three harmonic components. (e) The difference between raw receiver functions R and harmonic receiver functions H. (f) The raw receiver functions, The Gaussian coefficients of receiver functions are 1.0.

Methods

Due to the receiving function is extracted from the high-frequency teleseismic body wave signal (>0.5 Hz), and obviously affected by the tilting interface and anisotropy along the ray. While, the surface wave dispersion obtained from the ambient noise tomography has a lower frequency-band (<0.2 Hz), and depicts the averaged characteristic beneath each single parameterized space with a horizontal resolution scale related to the inter-station distance and wave-length. Therefore, we use three harmonic components (Shen et al., 2013), including back-azimuthally independent component, and two back-azimuthally dependent components with 2π and π periods, to fit the variation in amplitudes H(θ, t) of receiver functions at a specific time t (Figure 2). Obviously, the back-azimuthal independent component A0(t) represents the response of the horizontal layered isotropic structures beneath the station. And the piercing points of the Ps converted phases at the depth of 60 km are predominantly circular distribution centered at the station with a diameter of 0.5°, which is coordinate with the horizontal resolution scale of the Rayleigh wave phase and group velocity dispersions (0.5° × 0.5° grids) used in this study (Li et al., 2018a) . Therefore, the A0(t) is chosen as the average receiver function of the station, and used in joint inversion with Rayleigh wave group (6–42 s) and phase velocity (6–40 s) dispersions cubic spline interpolated at each station along the profile (Figure 3). Based on the CPS 3.30 software package (Herrmann, 2013), an iteratively damped least-squares algorithm is used to process the joint inversion of receiver functions and Rayleigh wave group and phase velocity dispersions to obtain the 1-D S-wave velocity structure beneath each station (Figure 4).

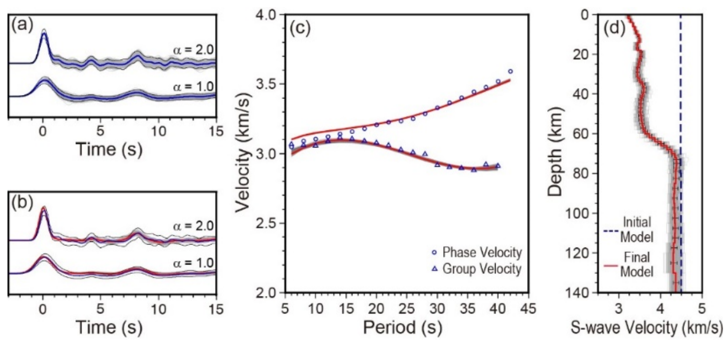

Figure 4. Examples of the joint inversion of receiver functions and surface wave dispersion.

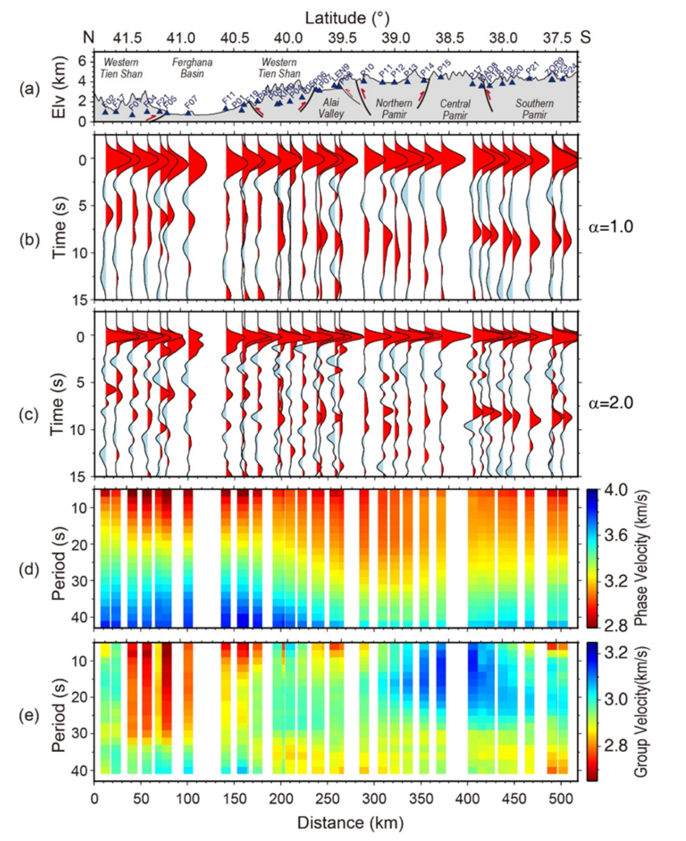

Figure 3. (a) Tectonics (black lines with red arrows) and stations (blue triangles with marks) are plotted with the topography along the profile. (b-c) The average receiver functions of each station along the profile with the Gaussian coefficients of 1.0 and 2.0. (d-e) The Rayleigh wave phase and group velocity dispersions of each station along the profile.

Results and Discussions

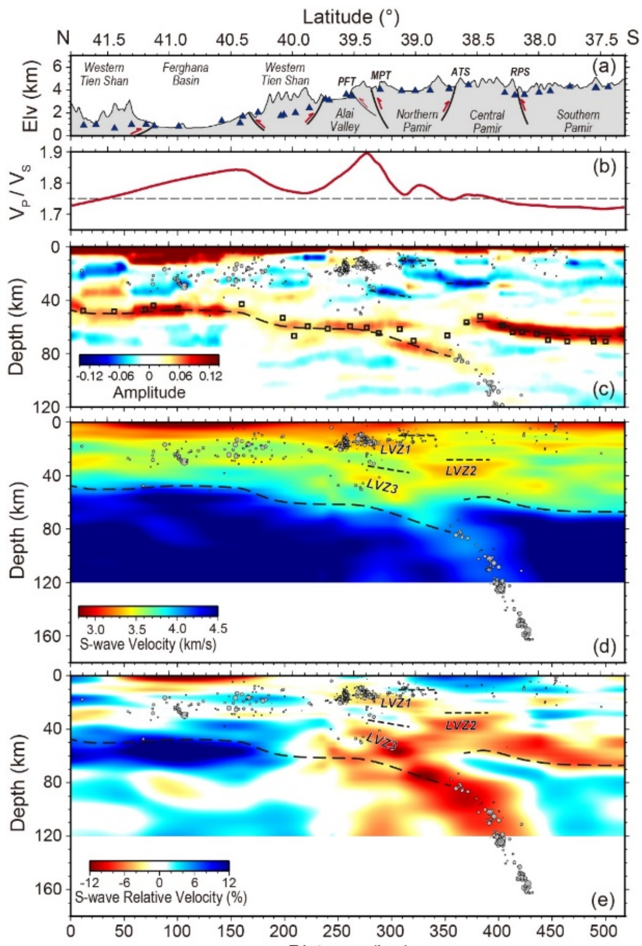

The 2-D S-wave velocity model along the profile obtained , and comprehensively combined with the CCP stacking image and crustal averaged V_P/V_S to depict the refined structures of the crust and uppermost mantle beneath the Pamir plateau (Figure 5). The intermediate-depth seismic zone is enveloping in a mantle LVZ which extends upward to the crustal bottom and connects with a lower crustal LVZ in the northern Pamir. And above it, another crustal LVZ is collocated with the uplift of the Moho. Therefore, we propose a conceptual model of the continental subduction beneath the Pamir plateau. In this model, the lower crust has deeply subducted with the lithospheric mantle as a response to the Indian–Eurasian continental collision. As the temperature-pressure condition will change with the depth increasing (> ~80 km), the dehydration embrittlement of the crustal materials will happen and cause the intermediate-depth seismicity beneath the Pamir plateau. And the fluids generated in this process will upward migrate into the overlaying slab through the mantle wedge or along the subduction channel, and enrich in the middle-lower crust to form two divided low-velocity anomalies above the intermediate-depth seismic zone (LVZ2) and at the tail of the subducting zone (LVZ3), respectively. The fluids enrichment and possibly hydrous melting will significantly reduce the middle-lower crustal strength and restrict the shallow tectonic deformation and seismicity in the brittle upper crust. The upper crustal LVZ1 in the northern margin of the plateau should be related to the brittle fractures caused by large-scale thrust faults restricted in the upper crust.(Figure 6).

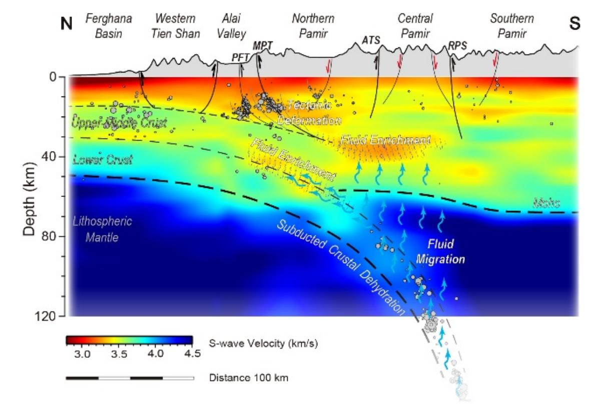

Figure 6. Interpreting section of the geodynamic processes of continental subduction.

Figure 5. (a) Tectonics and stations are plotted with the topography along the profile. (b) Crustal averaged V_P/V_S interpolated from the H-κ stacking results (Schneider et al., 2019). (c) The CCP stacking results of the quality controlled receiver functions with the Gaussian coefficient of 2.0. Black dashed lines represent the interpreted Moho and negative phases in the crust. Black squares denote the crustal thickness beneath the stations obtain from the H-κ stacking results (Schneider et al., 2019). Gray circles denote the earthquakes located within 25-km range on the both side of the profile (source: Sippl et al., 2013b; Kufner et al., 2017). (d) The absolute S-wave velocity structure obtained from the joint inversion of receiver functions and surface wave dispersions. (e) The relative S-wave velocity structure estimated with a reference to 1-D model average from the 2-D S-wave velocity structure in (d).

References

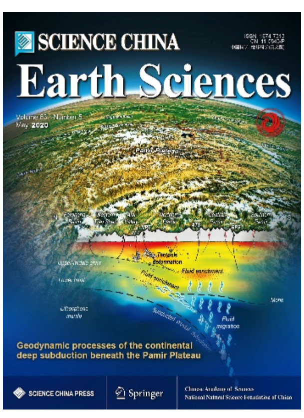

https://doi.org/10.1007/s11430-019-9587-3

- Chopin C. 1984. Coesite and pure pyrope in high-grade blueschists of the western Alps: A first record and some consequences. Contrib Mineral Petrol, 86: 107–118
- Herrmann R B. 2013. Computer programs in seismology: An evolving tool for instruction and research. Seismol Res Lett, 84: 1081–1088
- Kufner S-K, Schurr B, Haberland C, et al. 2017. Zooming into the Hindu Kush slab break-off: A rare glimpse on the terminal stage of subduction. Earth Planet Sci Lett, 461: 127–140
- Kufner S-K, Schurr B, Sippl C, et al. 2016. Deep India meets deep Asia: Lithospheric indentation, delamination and break-off under Pamir and Hindu Kush (Central Asia). Earth Planet Sci Lett, 435: 171–184
- Li W, Chen Y, Yuan X, et al. 2018a. Discrepant crustal deformation beneath the Pamir revealed by joint inversion of surface wave dispersion and receiver function. Washington, D. C.: Fall Meeting of American Geophysical Union
- Li W, Chen Y, Yuan X, et al. 2018b. Continental lithospheric subduction and intermediate-depth seismicity: Constraints from S-wave velocity structures in the Pamir and Hindu Kush. Earth Planet Sci Lett, 482: 478–489
- McKenzie D P, Jackson J A, Priestley K F. 2019. Continental collisions and the origin of subcrustal continental earthquakes. Can J Earth Sci, 56(11): 1101–1118
- Schneider F M, Yuan X, Schurr B, et al. 2013. Seismic imaging of subducting continental lower crust beneath the Pamir. Earth Planet Sci Lett, 375: 101–112
- Schneider F M, Yuan X, Schurr B, et al. 2019. The crust in the Pamir: Insights from receiver functions. J Geophys Res, 124: 9313–9331
- Shen W, Ritzwoller M H, Schulte-Pelkum V, et al. 2013. Joint inversion of surface wave dispersion and receiver functions: A Bayesian Monte-Carlo approach. Geophys J Int, 192: 807–836
- Sippl C, Schurr B, Tympel J, et al. 2013a. Deep burial of Asian continental crust beneath the Pamir imaged with local earthquake tomography. Earth Planet Sci Lett, 384: 165–177
- Sippl C, Schurr B, Yuan X, et al. 2013b. Geometry of the Pamir-Hindu Kush intermediate-depth earthquake zone from local seismic data. J Geophys Res, 118: 1438–1457
- Smith D C. 1984. Coesite in clinopyroxene in the caledonides and its implications for geodynamics. Nature, 310: 641–644
- Zheng Y F, Ye K, Zhang L F. 2009. Developing the plate tectonics from oceanic subduction to continental collision. Chin Sci Bull, 54: 2549–2555